Performance Estimation of Polarization Multiplexed DPSK Signal Transmission over Temporally Correlated Free Space Optical Channel

Abhishek Mani Shukla (abhishek.pee17@iitp.ac.in)
Indian Institute of Technology

Sumanta Gupta
Indian Institute of Technology

Research Article

Keywords: Stochastic Differential Equation (SDE), Mach-Zehnder Interferometer (MZI), Polarization Division Multiplexing (PDM)

Posted Date: February 24th, 2023

DOI: https://doi.org/10.21203/rs.3.rs-2611386/v1

Additional Declarations: No competing interests reported.

Version of Record: A version of this preprint was published at Optical and Quantum Electronics on June 30th, 2023. See the published version at https://doi.org/10.1007/s11082-023-05087-y.

Performance Estimation of Polarization Multiplexed DPSK Signal Transmission over Temporally Correlated Free Space Optical Channel

***Abhishek Mani Shukla · Sumanta Gupta**

Received: date / Accepted: date

Abstract The performance of polarization division-mul tiplexing (PDM) differential phase-shift keying (DPSK) modulated signal transmission over a slow varying turbulence channel is estimated in this paper. The turbulent free space optical channel is simulated using a stochastic differential equation (SDE)-based numerical channel simulator that takes into account the temporal correlation effect of the channel. The SDE-based channel simulator model may significantly ease the free space optical (FSO) communication system design since it enables the simulation of channel states according to predefined first- and second-order statistics, namely channel distribution and auto-covariance. We report the performance comparison of the PDM-DPSK system over an uncorrelated fast-varying FSO channel and a time-correlated slow-varying channel. Furthermore, to incorporate the effects of polarization and phase fluctuations in the FSO link, both time-dependent and Gaussian-distributed, simulated using SDE methods. The bit error rate (BER) performance obtained from the numerical simulation of the PDM-DPSK system shows that the impact of intensity fluctuations is more severe than polarization and phase fluctuation. The power penalty relative to back-to-back (B2B) is 0.5 dB, 2.5 dB, and 7 dB for a 1 km FSO link to achieve a threshold BER of 10^{-3} for weak, moderate, and strong turbulence conditions, respectively, for a slow varying turbulence channel. We find that for fast-changing turbulent channels, the PDM-DPSK link can not achieve the threshold BER value, particularly for medium and strong turbulence. For weak turbulence, 2 dB more received power is required to achieve the threshold BER value. Thus, the measured BER performances of the PDM-DPSK system over a fast-varying turbulent channel are overestimated, which does not provide the actual link performance over the time-correlated turbulent channel.

Keywords Stochastic Differential Equation (SDE), Mach-Zehnder Interferometer (MZI), Polarization Division Multiplexing (PDM)

A. M. Shukla *Corresponding author
Electrical Department,Indian Institute of Technology, Patna, India

E-mail: abhishek.pee17@iitp.ac.in

S. Gupta
Electrical Department,Indian Institute of Technology, Patna, India

E-mail: sumanta@iitp.ac.in

1 Introduction

Free-space optical (FSO) systems can provide high-data-rate, secure, and cost-effective communication links for applications such as wireless front- and backhauling for 5G and 6G networks [1][2]. Advancements in the Internet of Things (IoT), big data, and artificial intelligence (AI) in the area of technology requirement for high-speed connectivity with larger coverage area are the primary concern of the sixth-generation (6G) wireless communication [2]. Recently, many authors have proposed the satellite aerial ground integrated network (SAGIN) as a promising network architecture for future sixth-generation (6G) wireless communications[3]. In SAGIN, FSO communication is expected to be the key technology for providing extremely high-speed connectivity [3]. For terrestrial FSO communication, atmospheric turbulence can cause random changes in the received light intensity, directly impacting communication performance [4],[5], [6].

Commonly, On-Off Keying (OOK) modulated signals are used for FSO communication due to the simple receiver circuit and cost-effectiveness [7]. However, OOK-modulated signals are highly sensitive to atmospheric turbulence, and it needs adaptive thresholding to perform optimally[8]. In Binary phase shift keying (BPSK) and differential phase shift keying (DPSK) modulation formats information is engraved in phase. At the receiver end the DPSK signal can be demodulated by comparing the phases of two consecutive bits under a time-invariant channel [9], [10]. Unlike BPSK, which needs precise phase information over a bit and needs a phase noise compensation technique during demodulation, DPSK demodulation does not require precise phase estimation [11]. Moreover, the DPSK modulation technique requires no adaptive thresholding and offers a 3 dB better receiver sensitivity over OOK when detected with a self-homodyne delay interferometer and a balanced photo-detector. Thus DPSK can be power efficient and cost-effective for FSO communication links [8]. The BER performance of the DPSK modulated signal over the FSO channel was examined using the K-distributed turbulence model [9], and over Gamma-Gamma distributed atmospheric channels[12],[13], [14].

The strength of the turbulence in FSO channel is the function of the refractive index structure parameter(C_n^2), which depends on the temperature variation of the environment [5]and transversal wind velocity[5],[9],[10]. It is shown that the correlation time of the received signal strongly depends on the turbulence strength of the FSO link and as the strength of the turbulence increases, the correlation time decreases[15]. Thus, the turbulence in the FSO channel is a time-dependent process and varies slowly (in the order of milliseconds) with the environment temperature and wind velocity [16]. Previous studies did not consider the effect of the slowly varying nature of the turbulent channel which is very important for Gbps rate transmission as the FSO channel varies at kHz rate [15],[17], [18]. Moreover, works have reported the performances of the BPSK coherent polarization division multiplexed (PDM) systems for FSO communication[19] to increase transmission capacity. We have not found such work for DPSK transmission over the FSO link. Although in our recent work, we show that the differential detection technique can perform better than conventional direct detection techniques for a medium and strong turbulence channel condition over a slow varying turbulence channel for terrestrial communication[15]. So, there is a need to study the PDM- DPSK system over a slow varying FSO channel. As the PDM-DPSK transmission performance gets affected by polarization, phase, and intensity fluctuation, it is needed to take into account the variations of these parameters as well.The strength of the polarization and phase fluctuations are also the function of (C_n^2) value, so we can consider these fluctuations also time-dependent and varying slowly, similar to the turbulence channel states [12],[20], [21]. Thus for a Gbps rate FSO system, the turbulent channel coefficients remain constant for a block of bits [18] and a proper channel model needs to be implemented for estimating the performance of the PDM-DPSK system. The temporal irradiance fluctuation at the receiver has been observed in [9] and the temporally correlated Gamma-Gamma channel samples have been generated by using a time series generator. Considering the frozen atmosphere assumption the effect of phase noise and intensity fluctuation on DPSK modulated FSO system over correlated channels has been reported in [5], [22]. Although the methods used in the literature for generating the correlated channel samples are easy but not accurate and can not be used for PDM systems.

According to the author's best knowledge, no work has been reported on the performance study of the PDM-DPSK modulation-based FSO link using a stochastic differential equation (SDE) technique-based channel simulator, which is more efficient and accurate. This method, in particular, generates Gamma-Gamma and Gaussian distributed sample values using the exponential autocorrelation function with a predefined correlation time [23]. Using such a model may ease the design of communication systems since it enables the simulation of channel states according to predefined first- and second-order statistics, namely channel distribution, auto-covar iance, and power spectral density. In this paper, we have simulated the channel statistics using the SDE method under different turbulent conditions and estimated the performance of the PDM-DPSK link. Deviation in the performance estimation if the correlated channel model is not used is also reported. A simulation model to account for the combined effect of intensity, phase, and polarization fluctuations on the BER performance of the PDM-DPSK system is also discussed.

The remaining paper is structured as follows: Section 2 briefly discusses system model, and Section 3 FSO channel models. Section 4 and 5 discusses modeling of temporally correlated channel, and generation of PDM-DPSK signal, respectively. In Section 6, simulation results are presented. Concluding remarks are addressed in Section 7.

2 PDM-DPSK Transmission

2.1 System Model

The schematic block diagram of the PDM-DPSK-based FSO transmission system used for the simulation study is shown in Fig. 1. Two streams of orthogonally polarized lights are generated using a polarization beam splitter (PBS). Two different pseudo-random bit sequences (PRBS) are then modulated using two DPSK modulators with these orthogonally polarized light beams. Inside the DPSK modulator the data bits are differentially encoded by the delay-XOR pre-coder circuit [6]. Then, the pre-coded data sequence is modulated using the phase modulator. The DPSK modulated signal is given by[8];

$$\vec{E(t)} = E_0 e^{j\phi_s(t)}. \tag{1}$$

Where, ϕ_s is the phase difference between previous and current bit, E_0 is the amplitude of transmitted optical field. Then orthogonally polarized modulated signal is combined using polarization beam combiner and given to transmit optics. At the receiver side, the signal is received by receive optics and given to the erbium-doped fiber amplifier(EDFA) via variable optical attenuator (VOA), which control the input power of EDFA. EDFA amplifies the signal power level and also adds amplified spontaneous emission (ASE) noise. The ASE noise power is given by,

$$P_{ASE} = 2n_{sp}G\hbar\nu B \tag{2}$$

Where, n_{sp} is spontaneous emission coefficient, G is a linear gain of EDFA, $\hbar$ is Planck's coefficient, ν is frequency of light and B is the bandwidth of C band. The amplified signal is passed through an optical band-pass filter (OPBF) to limit ASE and background noise. Then the signal is fed into PBS which de-multiplex the x- and y- polarized signal. Mach-Zehnder Inteferometer (MZI) based demodulator, which introduces a one-bit delay in one of its arms. A balanced photodetector (BPD) to convert an optical signal into an electrical signal. The current after the BPD is given by;

$$I(t) = RE_0^2 hcos(\phi_s(t) - \phi_s(t - T_b)) \tag{3}$$

Where, R is responstivity of photo-diode, h is intensity fluctuation parameter.

3 FSO Channel Model

In this section, we discuss about geometric loss along with intensity, polarization, and phase fluctuations of the FSO channel.

3.1 Geometric Loss

In the FSO system, as the medium is unguided due to the diffraction property of light, the power received at the receiver optics is less, causing a significant transmission loss. The geometric loss in dB is given by [5],

$$L_G = -20log\left[\frac{D_R}{D_T + \theta_{div}L}\right] \tag{4}$$

Where, D_R and D_T are receiver and transmitter diameter respectively and θ_{div} is divergence angle.

3.2 Effect of Atmospheric Turbulence on Intensity

The most widely used theory for the measuring strength of turbulence is Kolmogorov which has given unit less Rytov variance parameter[4];

$$\sigma_I^2 = 1.23C_n^2 k^{\frac{7}{6}} L^{\frac{11}{6}} \tag{5}$$

where, σ_I^2 is also known as scintillation index, L is the length of link, $k = 2\pi/\lambda$ is wave number, λ is the wavelength, and C_n^2 is a measure of the strength of turbulence in the refractive index and known as the refractive index structure parameter with units of $m^{-2/3}$. The value C_n^2 range from 10^{-17} $m^{-2/3}$ or less for weak turbulence conditions up to 10^{-13} $m^{-2/3}$ or more for strong turbulence conditions [4],[25].
The distribution of intensity scintillation is modeled by the Gamma-Gamma probability distribution function (PDF), which appropriately models weak to strong turbulence regimes of the atmosphere [26].

$$f(h) = \frac{2(\alpha\beta)^{(\alpha+\beta)/2}}{\Gamma(\alpha)\Gamma(\beta)} h^{\frac{\alpha+\beta}{2}-1} K_{\alpha-\beta}(2\sqrt{\alpha\beta h}), h > 0 \tag{6}$$

where, α, β parameters are represents effective number of large scale cells and small scale cells of the scattering process whose mathematical expression can be found in [4], Γ is gamma function, $K_{\alpha-\beta}$ is modified Bessel function of the second kind of order $(\alpha - \beta)$, and h is normalized signal intensity .

3.3 Effect of Atmospheric Turbulence on Phase

The fluctuation in the phase of modulated signal induced by atmospheric turbulence is follows Gaussian distribution [12]. The theory behind phase fluctuation has already been discussed in paper [12] and experimentally verified in different mediums. The PDF of phase fluctuation $(\Delta\theta)$ is given by [12];

$$f(\Delta\theta) = \frac{1}{\sqrt{2\pi}\sigma_s} \exp\left(\frac{\Delta\theta^2}{2\sigma_s^2}\right) \tag{7}$$

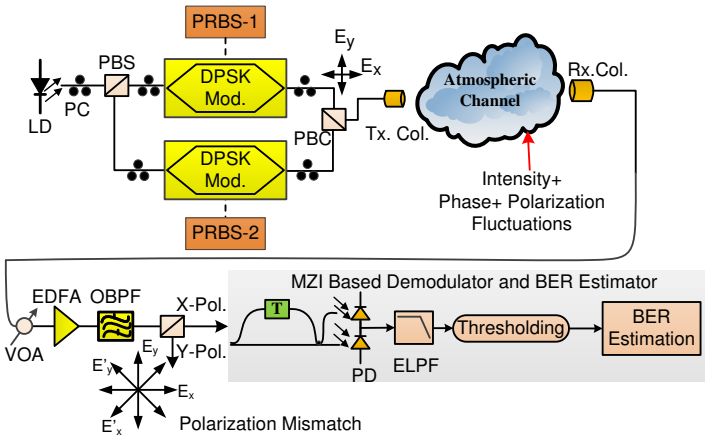

Fig. 1: Schematic Block diagram of PDM-DPSK based FSO system used for simulation, LD: Laser Diode, PC: Polarization Controller, PBS: Polarization Beam Splitter, PBC: Polarization Beam Combiner, Tx.: Transmitter, Col.: Collimator, Rx.: Receiver, VOA: Variable Optical Attenuator, EDFA: Erbium Doped Fiber Amplifier, OBPF: Optical Bandpass Filter, Pol.: Polarization, MZI: Mach-Zehnder Interferometer, PD: Photo-Diode, ELPF: Electrical Low Pass Filter.

Where, $\sigma_s^2 = 0.78 C_n^2 k^2 L_0^{\frac{5}{3}} L$ is the variance of phase for uniform propagation on single point and L_0 is outer scale parameter of turbulence.

3.4 Effect of Atmospheric Turbulence on Polarization Rotation

The PDM systems are susceptible to fluctuations in the state of polarization (SOP) and thus require polarization matching at both the transmitting and receiving ends [21] and affected by atmospheric turbulence, the amplitudes of the two orthogonally polarized lights experience different losses, leading to a change in the SOP [20]. J. Zhang et al. have studied the random fluctuations in the polarization angle of the light beam in turbulent media [21]. It is found that polarization fluctuation depends on the index of the refraction structure parameter, and the distribution of a received polarization angle is Gaussian in nature [20],[21]. For the PDM signal, the polarization rotation effect can be estimated by the amplitude received after PBS. The polarization rotation angle is $\Delta\Phi = \Phi(L) - \Phi(0)$ where $\Phi(L)$, and $\Phi(0)$ are the polarization angle at the receiver and source plane, respectively. If, E_x ,E_y are the two orthogonal optical fields received after PBS then polarization angle is estimated by [**?**];

$$\Delta\Phi = \tan^{-1}\left(\frac{\mid E_y \mid}{\mid E_x \mid}\right) \tag{8}$$

The relationship between polarization fluctuation and the index of the refraction structure parameter is given in [21]. The PDF expression of the received polarization angle fluctuation is given by [21];

$$f_{pol}(\Delta\Phi) = \frac{1}{\sqrt{2\pi}\sigma_\Phi} \exp\left(-\frac{\Delta\Phi}{2\sigma_\Phi^2}\right) \tag{9}$$

Where, $\sigma_\Phi = \frac{(C_n^2)^{\frac{1}{2}} \lambda^{\frac{7}{6}} L^{\frac{2}{3}}}{2\sqrt{2}\pi^{\frac{3}{4}} l^{\frac{3}{2}}}$ and l is scale factor.

4 Modeling of Temporally Correlated Channel

The numerical technique used in the paper [23] for generating Gamma-Gamma channel states with an exponential auto-correlation function is efficient and accurate. It addresses the effect of temporal covariance with a predefined correlation time, and by repeated calculation of a discrete differential equation, the states of the channel can be generated. The parameters used for the generation of temporally correlated channel states are the distribution parameter and the white Gaussian noise (WGN) sequence [23]. This method is based on the numerical solution of the first-order SDE.

4.1 Generation of Gaussian Distributed Channel Coefficient

The temporally correlated Gaussian distribution has been generated by using the method given below. The first order SDE is given by [24],

$$\frac{dx}{dt} = p(x) + q(x)\xi(t) \tag{10}$$

where, $p(x)$ and $q(x)$ are drift and diffusion function. For a Gaussian process with exponential auto-correlation function, the $p(x)$ and $q(x)$ are given in ([28], Eq.(48), (50)). The values of $p(x)$ and $q(x)$ for Gaussian process with correlation time τ_c are given by [27] ;

$$p(x) = -\frac{x}{\tau_c}, \quad q(x) = \frac{2\sigma^2}{\tau_c} \tag{11}$$

By using the solution of stochastic differential equation given by ([23], Eq.(13)), and putting the values of $p(x)$ and $q(x)$ discrete time differential equation for Gaussian process is given by;

$$x_{k+1} = x_k - \frac{(x_k - \mu)}{\tau_c}\Delta t + \sqrt{\frac{2\sigma^2 \Delta t}{\tau_c}}\xi_k. \tag{12}$$

Where μ, σ^2 are mean and variance of the known pdf respectively. Indexes k, $k+1$ are related to values at time t_k, and t_{k+1} respectively. $\xi(t)$ is normally uncorrelated WGN process and Δt is channel sampling period. Fig.2 (a) shows the samples of temporally-correlated Gaussian process has generated using Eq.12 with $\tau_c =$ 5 ms, channel sampling period 10^{-4} sec, $\mu = 0$ and $\sigma = 2.0398$. The normalized histogram of the temporally correlated Gaussian samples is shown in Fig.2 (a). Here the analytic Gaussian PDF is also plotted and it is found that the normalized histogram matches well with the analytical PDF.

4.2 Generation of Gamma-Gamma Distributed Channel Coefficient

Solving SDE samples of temporally correlated Gamma distributed process are generated. The general expression of discrete time differential equation for Gamma channel simulator with a predefined correlation time τ_c is given by [23];

$$x_{k+1} = \frac{x_k \tau_c + \alpha\Theta\Delta t + \Theta\Delta t(\xi_k^2 - 1)/2 + [2x_k\Theta\tau_c\Delta t]^{1/2}\xi_k}{\tau_c + \Delta t} \tag{13}$$

The two different Gamma distribution can be obtained by using Eq.13 putting $\Theta = 1/\alpha$ and $\Theta = 1/\beta$. If x_k, y_k are two Gamma process with parameters α, β and correlation time τ_c, then Gamma-Gamma process can be obtained by the multiplication of two Gamma distribution solution,

$$h_k = x_k y_k, \forall k. \tag{14}$$

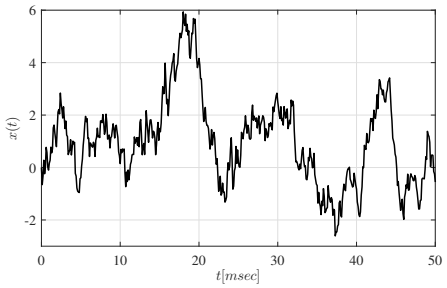

(a)

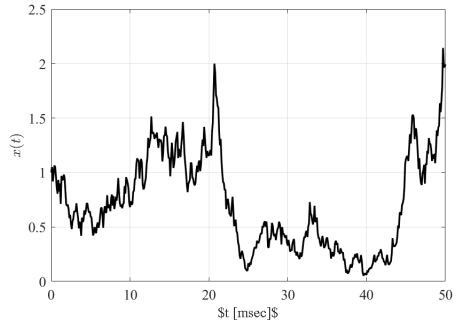

(b)

Fig. 2: (a) Time Correlated Gaussian process for $\tau_c = 5$ ms, (b) Temporally-correlated samples of the Gamma process for $\tau_c = 5$ms.

Fig. 2(b) shows samples of temporally correlated Gamma distributed process with $\tau_c = 5$ ms and $\alpha = 5$. The normalized histogram of the samples and the analytic PDF are shown in Fig.3 (b). Results indeed show that the PDF of the generated samples matches well with the analytic PDF.

5 Transmitter and Receiver Modeling for PDM-DPSK Signal

5.1 Transmitter

At transmitting end as shown in Fig.1, two data PRBS (with maximal length $2^{31} - 1$ and $2^{23} - 1$) are modulated by the DPSK modulator using two orthogonal polarized light beams. Then both orthogonally polarized light beams are combined by a polarization beams combiner (PBC) and transmitted to free space sharing the same bandwidth and carrier frequency. The polarized baseband optical field is given by;

$$E_{tx}(t) = E_0 e^{j\phi_{sx}(t)}\hat{x}, \quad E_{ty}(t) = E_0 e^{j\phi_{sy}(t)}\hat{y}. \tag{15}$$

Where, $E_t = [E_{tx}; E_{ty}]'$ is transmitted signal vector of 2×1 and $\hat{x}, \hat{y}$ represents the SOP at the output of PBC

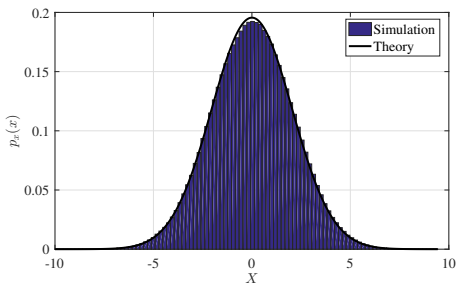

(a)

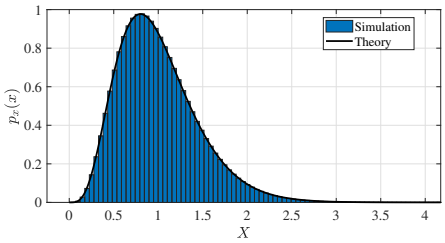

(b)

Fig. 3: (a) The analytic PDF and the normalized histogram of the generated temporally correlated Gaussian samples $\tau_c = 5$ ms, (b) The analytic PDF and the normalized histogram of the generated temporally correlated Gamma samples $\tau_c = 5$ ms.

aligned with $\hat{x}$ and $\hat{y}$ axis. ϕ_{sx} and ϕ_{sy} are the signal phase for x and y-polarized signals, respectively. Here it is assumed that the amplitudes of both polarizations are equal. For an effective communication system, the polarization rotation effect rotates the axis of polarization by angle $\Delta\phi$. Then a new axis of polarization became $\hat{x'}$ and $\hat{y'}$ as shown in Fig.1.

5.2 Receiver

At receiving end, the signal received by receive optics is given to PBS which demultiplex the signal into x and y polarization as shown in Fig.1. The polarization rotation effect, along with phase and amplitude fluctuation affected the received signal $E_r = [E_{rx}; E_{ry}]'$. The two components of the received signal coming out of the two ports of the PBS are given by;

$$\begin{aligned} E_{rx}(t) &= E_0 h[cos(\Delta\Phi) - sin(\Delta\Phi)]e^{j(\phi_{sx}(t)+\Delta\theta)}, \\ E_{ry}(t) &= E_0 h[cos(\Delta\Phi) + sin(\Delta\Phi)]e^{j(\phi_{sy}(t)+\Delta\theta)}. \end{aligned} \tag{16}$$

Each polarized signal is demodulated by a delay-MZI based demodulator as shown in Fig.1. The expression for output current following a balance photo-detector and electrical low pass filter (ELPF) for the optical signal coming out of the x-polarized port of PBS can be given by,

$$\begin{aligned} i_x = RE_0^2 h[&cos^2(\Delta\Phi)cos(\phi_{sx}(t) - \phi_{sx}(t - T_b)) \\ &+ sin^2(\Delta\Phi)cos(\phi_{sy}(t) - \phi_{sy}(t - T_b)) \\ &- sin(\Delta\Phi)cos(\Delta\Phi)\big(cos(\phi_{sx}(t) - \phi_{sy}(t - T_b)) \\ &+ cos(\phi_{sx}(t - T_b) - \phi_{sy}(t))\big)] + n_x. \end{aligned} \tag{17}$$

Where, n_x is the additive white Gaussian(AWGN). T_b is the bit period, R is the responsivity of the photodetectors in BPD and h is the channel gain. Similarly, we can obtain the current, i_y at the output for the optical field coming out from the y-port of the PBS.

Table 1: List of Parameters and Constants

Name	Symbol	value
Wavelength	λ	1550 nm
Data-rate	R_b	1 Gb/s
Responsivity	R	1
Boltzmann constant	k_B	1.38×10^{-23} J/K
Electron charge	q	1.69×10^{-19} C
Outer scale parameter	L_0	10 m
Scale factor	l	10^{-8}
Channel sampling period	Δt	10^{-4} sec
Correlation time	τ_c	$1 - 10$ ms
Transmitter Diameter	D_T	0.08 m
Receiver Diameter	D_R	0.1 m
Divergence Angle	θ_{div}	0.001 radian
EDFA Gain	G	30 dB

6 Simulation Results and Discussions

In this section, we discuss the numerical simulation results of the PDM-DPSK-based FSO system performance over the different atmospheric scenarios at a data rate of 1 Gb/s. The values of the parameters and constants used in the simulation study are given in Table-1. The temporally correlated channel coefficients are simulated for weak, medium, and strong turbulence for correlation times of 5 ms, 3 ms, and 1 ms, respectively, using the numerical method discussed above. The data rate of 1 Gbps is chosen to reduce the simulation time, as a higher data rate needs more bits to transmit through the channel to capture the slowly varying nature of the FSO channel. We strongly believe that the simulation method is even applicable for higher data rates as well. For the estimation of BER, the total time window for simulation is taken at least ten times the correlation time. The BER values are reported only when the bits in error exceed 100. The performance of

Table 2: Parameters for Simulating Different Turbulent Conditions

Parameters Name	Weak Turb.	Medium Turb.	Strong Turb.
C_n^2 (in $m^{-2/3}$)	5×10^{-16}	5×10^{-15}	5×10^{-14}
τ_c (in ms)	5	3	1
σ_s (in radian)	0.1724	0.5451	0.7710
σ_ϕ (in radian)	0.0420	0.0747	0.0889
σ_I	0.0998	0.3155	0.9977

only the x-polarized signal is estimated as other polarization behave similarly. Power penalties are estimated at the target BER of 10^{-3} as the 7%-over head FEC requires 3.8×10^{-3} of BER value.

Fig. 4 shows the BER performance of the PDM-DPSK channel for an x-polarized signal after 1 km of link length. The weak turbulence condition is simulated by considering the parameters listed in Table-2. To estimate the effect of intensity, phase, and polarization fluctuation we have simulated three different scenarios; (i) link affected by only intensity fluctuation, (ii) link affected by both intensity and phase fluctuations, and (iii) link affected by intensity, phase, and polarization fluctuation. It is to be noted that only the third scenario will be observed in practice. Under correlated channel conditions, the results show that intensity fluctuation is the main contributor to the BER degradation; whereas phase and polarization fluctuations play an insignificant role. This is due to the quasi-static nature of the turbulence for the bit period. The phase and intensity barely change between two bits, which are having 1 ns of durations. The results show that in presence of intensity, phase, and polarization fluctuation around 0.5 dB of power penalty is estimated at a BER value of 10^{-3} when compared to the back-to-back condition.
In Fig. 4 we also plot the BER performance for the uncorrelated channel, which is simulated with similar parameters as listed in Table-1 but only the correlation time is made negligibly small. Under this situation the intensity, phase, and polarization change in each bit. It is observed that in the uncorrelated channel, the performance of PDM-DPSK becomes worse than the correlated channel, making the power penalty at 10^{-3} BER equal to 2.5 dB (2 dB more than the correlated channel). Moreover, we also observe that a slightly more penalty is observed when both intensity and phase fluctuations are considered, compared to only intensity fluctuation conditions. Thus we infer that the simulation of the uncorrelated channel will overestimate the BER values, whereas the actual system may perform better.

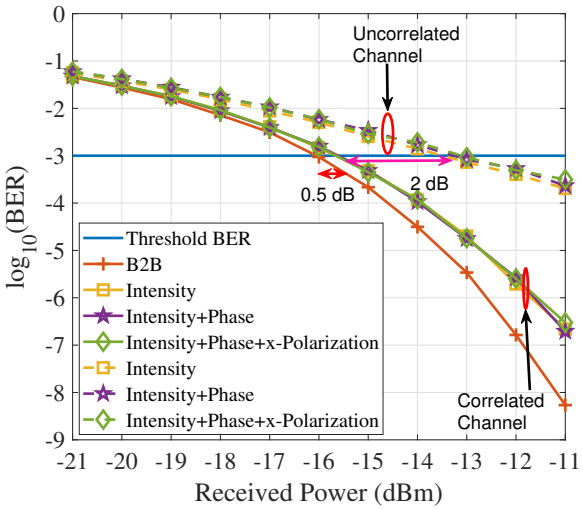

Fig. 4: BER. Vs received power in weak turbulence for 1km. The solid line is for the correlated channel and the dashed line is for the uncorrelated channel.

In Fig.5, we show the BER performance of 1 Gbps/ polarization DPSK signal transmission over a 1 km FSO link under medium turbulence conditions. The BER performances are estimated in the presence of intensity, intensity+phase, and intensity+phase+polarization fluctuations for both correlated and uncorrelated channels. The channel parameters are listed in Table-2. From the BER results it is observed that the uncorrelated channel model is not at all suitable for BER estimation as it fails to achieve the required BER of 10^{-3}. For the temporally correlated channel in presence of fluctuations from all three parameters, the estimated power penalty at 10^{-3} BER is found to be 2.5 dB. Moreover, it is seen that the BER penalty is mainly contributed by intensity fluctuation as the phase and polarization do not change between two consecutive bits in a temporally correlated channel.

Fig. 6 shows the BER performance under strong turbulence in a 1 km FSO link. The estimated power penalty is found to be 7 dB at a BER of 10^{-3}. Similar to the medium turbulence condition, under strong turbulence also uncorrelated channel model fails to achieve a BER of 10^{-3}. From the performance estimation of PDM-DPSK signal transmission, it is concluded that consideration of temporally correlated channels is essential. Else the BER values get overestimated. Moreover, our presented SDE-based channel simulator can be beneficial for emulating different temporally correlated channels.

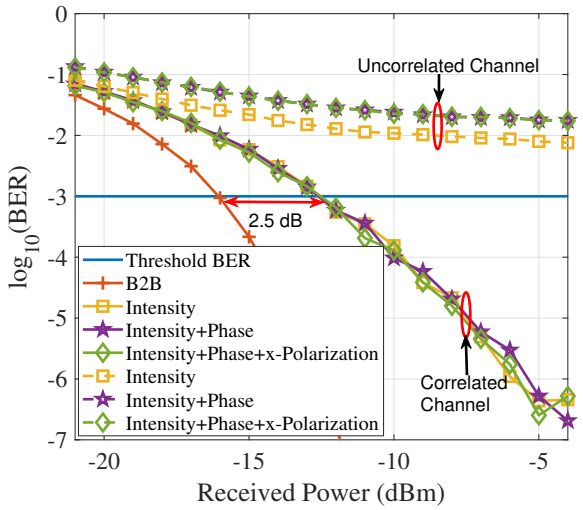

Fig. 5: BER. Vs received power in medium turbulence for 1 km. The solid line is for the correlated channel and the dashed line is for the uncorrelated channel.

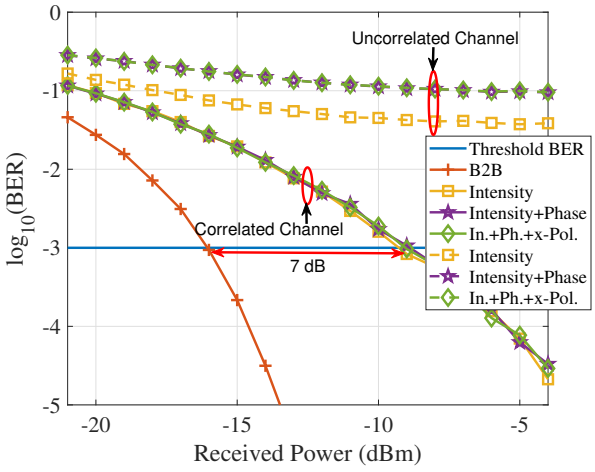

Fig. 6: BER.Vs received power in strong turbulence for 1km. The solid line is for the correlated channel and the dashed line is for the uncorrelated channel.

7 Conclusions

In this paper, we report the performance of the PDM-DPSK-based FSO link over the temporally correlated turbulent channels, which are simulated by using the SDE-based numerical method. In this study, we consider the effect of intensity, polarization, and phase fluctuations. Temporally correlated Gaussian and Gamma-Gamma distributed samples are generated by solving the SDE with predefined correlation times. These are then used to simulate the phase, polarization, and intensity fluctuation of a turbulent FSO link having a length of 1km. To compare the performance of the temporally correlated channel with the uncorrelated channel responses are also simulated considering fast fluctuation. The BER results show that the performance of the PDM-DPSK signal over the FSO link is highly dependent upon the atmospheric turbulence; as the strength of turbulence increases, the power penalty also increases. Moreover, results also reveal that the effect of polarization and phase fluctuation on the PDM-DPSK-based FSO link is negligible over different turbulence conditions when compared to the intensity fluctuation. The results also indicate that the BER values are overestimated over the fast-varying channel. Simulation results show the power penalties at BER of 10^{-3} for weak, medium, and strong turbulence are 0.5 dB, 2.5 dB, and 7 dB, respectively. Whereas under medium and strong turbulent conditions the PDM-DPSK system fails to achieve the BER of 10^{-3} when fast varying uncorrelated channel models are considered.

Declarations

Author Contributions All authors contributed to the study conception and design. Analysis were performed by A M Shukla. The first draft of the manuscript was written by A M Shukla. S Gupta reviewed and commented on final manuscript.

Funding Not applicable.

Availability of data and materials The datasets generated during and/or analyzed during the current study are available from the corresponding author on reasonable request.

Conflict of interest The authors declare that they have no known competing financial interests or personal relationships that could have appeared to influence the work reported in this paper.

Ethical approval Not Applicable (N/A).

References

1. Jeon HB, Kim SM, Moon HJ, Kwon DH, Lee JW, Chung JM, Han SK, Chae CB, Alouini MS (2022) Free-space optical communications for 6g-enabled long-range wireless networks: Challenges, opportunities, and prototype validation. arXiv preprint arXiv:220907674.
2. Viswanathan H, Mogensen PE (2020) Communications in the 6g era. IEEE Access 8:57063–57074.
3. Nguyen TV, Le HD, Pham AT (2022) On the design of ris-uav relay-assisted hybrid fso/rf satellite-aerial-ground integrated network. IEEE Transactions on Aerospace and Electronic Systems.
4. Al-Habash A, Andrews LC, Phillips RL (2001) Mathematical model for the irradiance probability density function of a laser beam propagating through turbulent media. Optical Engineering 40(8):1554–1563.

5. Andrews LC, Phillips RL, Hopen CY (2001) Laser beam scintillation with applications, vol 99. SPIE press.
6. Chan VW (2006) Free-space optical communications. Journal of Lightwave technology 24(12):4750–4762.
7. Ghassemlooy Z, Tang X, Rajbhandari S (2012) Experimental investigation of polarisation modulated free space optical communication with direct detection in a turbulence channel. IET communications 6(11):1489–1494.
8. Ho KP (2005) Phase-modulated optical communication systems. Springer Science &Business Media.
9. Xie G, Dang A, Guo H (2011) Effects of atmosphere dominated phase fluctuation and intensity scintillation to dpsk system. In: 2011 IEEE International Conference on Communications (ICC), IEEE, pp 1–6.
10. Xu Z, Xu G, Zheng Z (2021) Ber and channel capacity performance of an fso communication system over atmospheric turbulence with different types of noise. Sensors 21(10):3454.
11. Li K, Lin B, Ma J (2020) Dpsk modulated multiple apertures receiver system for satellite-to-ground heterodyne optical communication. Optics Communications 454:124466.
12. Zhang J, Li R, Dang A (2015) Experimental studies of phase fluctuations in free-space optical communications. In: Applications of Lasers for Sensing and Free Space Communications, Optical Society of America, pp LTh2D–3.
13. Li M, Li B, Zhang X, Song Y, Chang L, Chen Y (2016) Investigation of the phase fluctuation effect on the ber performance of dpsk space downlink optical communication system on fluctuation channel. Optics Communications 366:248–252.
14. Tsiftsis T (2008) Performance of heterodyne wireless optical communication systems over gamma-gamma atmospheric turbulence channels. Electronics Letters 44(5):1.
15. Shukla AM, Gupta S (2022) Experimental demonstration: Differential detection of 10 gbps optical ook signal over turbulent channel. Optik 266:169564.
16. Tripathi A, Soni GG, Gupta S, Mandloi AS (2019) Experimental investigation of wind and temperature induced scintillation effect on optical wireless communication link. Optik 178:1248–1254.
17. Nguyen TV, Le HD, Dang NT, Pham AT (2021) On the design of rate adaptation for relay-assisted satellite hybrid fso/rf systems. IEEE Photonics Journal 14(1):1–11.
18. Shin WH, Choi JY, Han SK (2019) Fixed threshold on-off keying differential detection for satellite optical communications. Optics Express 27(2):1590–1596.
19. Zhou H, Xie W, Zhang L, Bai Y, Wei W, Dong Y (2019) Performance analysis of fso coherent bpsk systems over rician turbulence channel with pointing errors. Optics Express 27(19):27062–27075.
20. Shukla AM, Gupta S (2020) Simultaneous measurement of atmospheric turbulence induced intensity and polarization fluctuation for free space optical communication. In: 2020 National Conference on Communications (NCC), IEEE, pp 1–4.
21. Zhang J, Ding S, Zhai H, Dang A (2014) Theoretical and experimental studies of polarization fluctuations over atmospheric turbulent channels for wireless optical communication systems. Optics express 22(26):32482–32488.
22. Anguita JA, Cisternas JE (2010) Turbulence strength and temporal correlation in a terrestrial laser communication link. In: Free-Space Laser Communications X, International Society for Optics and Photonics, vol 7814, p 78140H.
23. Bykhovsky D (2016) Simple generation of gamma, gamma–gamma, and k distributions with exponential autocorrelation function. Journal of Lightwave Technology 34(9):2106–2110.
24. Bykhovsky D (2015) Free-space optical channel simulator for weak-turbulence conditions. Applied optics 54(31):9055–9059.
25. Ghassemlooy Z, Popoola W, Rajbhandari S (2019) Optical wireless communications: system and channel modelling with Matlab® CRC press.
26. Khalighi MA, Uysal M (2014) Survey on free space optical communication: A communication theory perspective. IEEE communications surveys & tutorials 16(4):2231–2258.
27. Kontorovich VY, Lyandres VZ (1995) Stochastic differential equations: an approach to the generation of continuous non-gaussian processes. IEEE Transactions on Signal Processing 43(10):2372–2385.
28. Primak S, Lyandres V, Kontorovich V (2001) Markov models of non-gaussian exponentially correlated processes and their applications. Physical Review E 63(6):061103.